scientific reports

Check for updates

OPEN

In vivo evaluation of tissue damage from varying grasping forces using the Saroa surgical system

Hiroyasu Nakashima[1]✉, Yuichiro Ueda[1], Yoko Miyanari[1], Teruyuki Nishihara[2], Makoto Hamasaki[3], Makoto Ohbu[4], Kenji Kawashima[5], Hajime Yamakage[6], So Miyahara[1], Keita Tokuishi[1], Ryuichi Waseda[1], Takeshi Shiraishi[1] & Toshihiko Sato[1]

Robot-assisted surgery can help to reduce patient burden and operator stress by enabling precise manipulations with multiple joint motions, but may also cause complications due to the lack of tactile sensation. The Saroa surgical system was developed with a haptic feedback function, and allows operators to adjust grasping forces as desired. In this study, we investigated tissue damage from varying grasping forces using the Saroa surgical system, and assessed the utility of this system. The grasping forceps of the Saroa system were used to grasp the lungs, esophagus, aorta, liver, spleen, small intestine, and large intestine of six beagle dogs with forces of 1, 2, and 3 N for durations of 1, 2, and 4 min. The effects of different grasping forces and durations on tissue damage were histologically evaluated. Histological evaluations showed that grasping force caused tissue damage in the lung and liver, but not the other organs. These results showed the lung and liver were more vulnerable to grasping forces, and exhibited more severe tissue damage at higher forces. These findings suggest that the haptic feedback function of the Saroa system could help to reduce intraoperative organ damage, especially in the fields of lung and liver surgery.

Keywords Grasping force, Tissue damage, Pneumatic surgical robot, Tactile sensation, Haptic feedback

Abbreviations

EVG	Elastica van Gieson
H&E	Hematoxylin and eosin
PAS	Periodic acid-Schiff
RAS	Robot-assisted surgery
RBC	Red blood cell
Saroa	Surgical Assist Robot by Air

The first "robotic surgeon" used on a human patient was the Programmable Universal Machine for Assembly (PUMA) 200, which was employed by Kwoh et al. in 1985 to perform a brain tumor biopsy[1]. However, this robot required pre-programming with fixed anatomical landmarks in each patient, and could not be used for dynamic surgical targets. In addition to such pre-programmable robotic surgeons, master-slave robots and robotic endoscope positioning systems have also been developed[2–5]. Robot-assisted surgery (RAS) has since become widely used in various surgical specialties, especially cancer surgeries[6]. The Da Vinci Surgical System (Intuitive Surgical, CA, USA) was launched as a master-slave robot in 1999[7], and has been employed in over 14 million patients worldwide[8]. In the field of thoracic surgery, a meta-analysis found that RAS produced short-term and long-term outcomes that were comparable to those of video-assisted surgery in patients who underwent lobectomy or segmentectomy for non-small cell lung cancer[9]. Although RAS is reported to reduce patient burden and operator stress by enabling precise manipulations with multiple joint motions[3,10,11], traditional open or endoscopic surgeries continue to be widely preferred due to RAS's high equipment costs, need for wide operating spaces, need for additional training and certifications, and lack of tactile sensation[12]. In particular, the lack of tactile sensation can prolong operative times and increase learning curves, thereby elevating the risk of

[1]Department of Thoracic, Breast and Endocrine, and Pediatric Surgery, Fukuoka University School of Medicine, 7-45-1 Nanakuma, Jonan-ku, Fukuoka 814-0180, Japan. [2]Riverfield Inc., Tokyo, Japan. [3]Department of Pathology, Fukuoka University School of Medicine, Fukuoka, Japan. [4]Department of Pathology, Kitasato University Kitasato Institute Hospital, Tokyo, Japan. [5]Department of Information Physics and Computing, School of Information Science and Technology, The University of Tokyo, Tokyo, Japan. [6]Department of Medical Statistics, Satista Co., Ltd., Kyoto, Japan. ✉email: nhs47.nakashima@gmail.com

surgical errors[13,14]. Moreover, robotic systems can generate forces that exceed tissue tolerance, resulting in tissue damage and potentially serious adverse events[15,16].

To compensate for the lack of tactile sensation, the Surgical Assist Robot by Air (Saroa) was developed with a haptic feedback function. This function is achieved through the use of pneumatically driven multi-degree-of-freedom forceps with a rigid-link mechanism and reduced motion interference between joints[17]. This system facilitates external force estimation by utilizing the high back-drivability of pneumatic cylinders, which allows operators to freely set upper limits to grasping forces and manipulate tissue with appropriate force[17]. Haptic feedback refers to the real-time re-creation and transmission of forces exerted on surgical instruments to the operating surgeon. To achieve this, it is necessary to quantify the force imparted on the forceps tips, transduce this mechanical load into electrical signals, relay these signals, and re-create the original forceps tip force at the master controller. Although achieving realistic haptic feedback remains a challenge in clinical applications, two principal methodologies have emerged as potential solutions. The first involves embedding miniaturized force sensors directly into surgical instrument tips to quantify localized forces[18]. The second entails quantifying the forces imparted along the instrument by the robotic arm itself, which can reduce instrument size and lower manufacturing costs relative to the first approach. This technique was pioneered in the Saroa surgical system, which became the first RAS platform integrated with a haptic force feedback mechanism for clinical use[17].

Studies have described various RAS-related complications resulting from issues such as patient positioning, robot malfunction, and lack of tactile sensation[13,15,19–25]. Our previous study demonstrated that tissue could be grasped with lower forces when using the haptic feedback function of the Saroa surgical system[26]. The present study investigated the degree of tissue damage for various organs according to grasping force and duration using the Saroa surgical system. Herein, we assess the usefulness of low grasping force for reducing tissue damage, and examine the potential utility of this system.

Materials and methods

Robotic system

Saroa is a pneumatically actuated robotic system developed by Riverfield Inc. (Tokyo, Japan), and was designed to provide real-time haptic feedback to the operating surgeon. Pneumatic cylinders within the robotic arms are utilized to actuate wires housed in each instrument, and these wires are subsequently linked to a fenestrated grasping jaw located at the instrument's tip (Fig. 1). The grasping force exerted at the jaw is generated by the pressure within these cylinders. This pressure is continuously monitored, with measured values translated into electrical signals that are transmitted to the hand controller; this facilitates real-time control and feedback of force. Saroa accurately estimates grasping forces with errors of less than 20% in comparison to the maximum output forces. Moreover, the practical sensitivity of external force estimation is >0.5 N. Grasping force is displayed on the console's sub-monitor and can be adjusted in real time, allowing the operator to vary the load while performing manipulations within the range of applicable force.

Animal experimental protocol

The study used six adult male beagle dogs weighing 8.06 to 9.08 kg provided from Kitayama Labes Co., Ltd. All animals received humane care in compliance with the "Guide for the Care and Use of Laboratory Animals" published by the US National Institutes of Health (NIH Publication No. 85-3, revised 1985). the study is reported in accordance with ARRIVE guidelines (https://arriveguidelines.org). The experimental protocol was approved by the Animal Experimental Committee of Fukuoka University (Approval No. 2214090). Each dog was sedated with an intramuscular injection of 0.05 mg/kg atropine sulfate, 10 mg/kg ketamine hydrochloride, and 7 mg/kg xylazine before being intubated with an 8-mm endotracheal tube. Anesthesia during mechanical ventilation was maintained using inhalational sevoflurane. After thoracotomy and laparotomy, the fenestrated grasping forceps of the Saroa surgical system were used to grasp the lungs, esophagus, aorta, liver, spleen, small intestine, and large intestine with forces of 1, 2, and 3 N for durations of 1, 2, and 4 min (Fig. 2). The dogs were euthanized deep anesthesia with an overdose of thiopental Sodium. The effects of these different grasping forces on the various tissues were examined. Surgically resected specimens were fixed in 10% formalin (room temperature for 24 h)

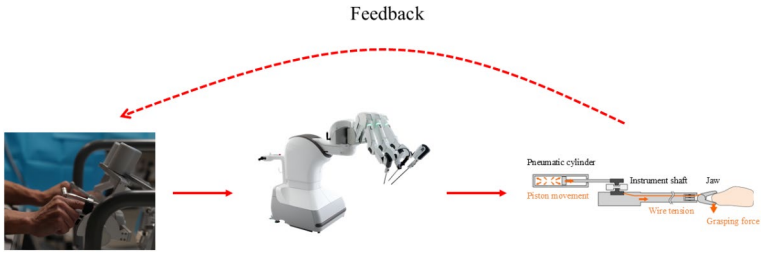

Fig. 1. Overview of the Saroa surgical system's feedback mechanism. This system can be grasped with lower forces when the haptic feedback function is engaged.

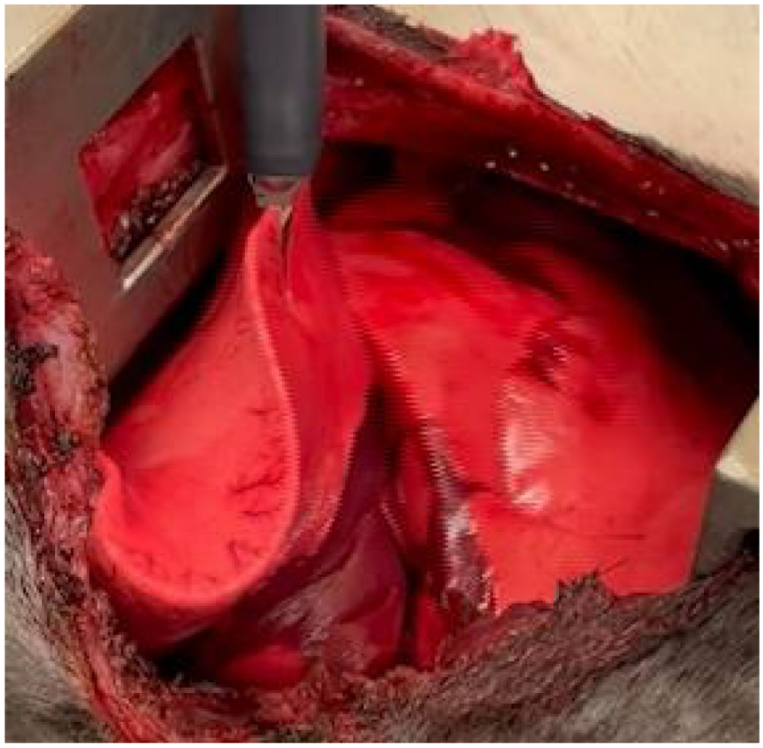

Fig. 2. Animal experiment. The photograph shows the lung of a beagle dog being grasped by the fenestrated grasping forceps of the Saroa surgical system.

and embedded in paraffin blocks. Tissue sections were cut at a thickness of 4 mm. Hematoxylin and eosin (H&E) staining, Elastica van Gieson (EVG) staining, and Periodic acid-Schiff (PAS) staining were performed.

Histological evaluation of tissue damage

Tissue damage was assessed under a microscope by two pathologists. The lungs were examined for the presence or absence of hemorrhage and congestion, and changes in alveoli, pleural elastic layers, and collagen layers. The liver and spleen were examined for the presence or absence of hemorrhage and congestion, and degeneration. The gastrointestinal tract was examined for the presence or absence of hemorrhage and congestion, and mucosal erosion. Aortic tissue was examined for the presence or absence of hemorrhage and congestion, and changes in elastic layers.

Measurement of areas of tissue damage

The areas of tissue damage were imaged using microscope and measured using BX-analyzer (BZ-X700, KEYENCE, Osaka, Japan). Organ parenchyma was recognized in yellow, erythrocytes in blue, pleural elastic layer in blue, and pleural collagen layer in blue. For lung tissue, we measured the area of hemorrhage and/ or congestion, red blood cell (RBC) count, and thickness of the pleural elastic layers and collagen layers. For liver and spleen tissue, we measured the area of hemorrhage and/ or congestion, RBC count, and area of degeneration. For gastrointestinal tract tissue, we measured the area of hemorrhage and/ or congestion, RBC count, and area of mucosal erosion. For aortic tissue, we measured the RBC count and elastic layer thickness in the intima, media, and adventitia.

Statistical analysis

Linear regression analyses were conducted to evaluate the associations between tissue damage and grasping forces. The regression models were constructed with tissue damage as the dependent variable and grasping force as the independent variable. The associations were evaluated by calculating standardized regression coefficients (β) and R^2 value. Statistical analyses were performed using JMP version 14.0 statistical software package for Windows (SAS Institute, NC, USA). A p-value of less than 0.05 was considered statistically significant. In addition, the post hoc power analysis was performed to evaluate the adequacy of the sample size. A power exceeding 0.8 was considered indicative of a sufficient sample size.

Results

Macroscopic findings

Macroscopic examination of the lung and liver revealed hemorrhage and congestion in grasped areas that increased with higher grasping forces (Fig. 3), but not with longer grasping durations. No macroscopic differences were detected in the esophagus, aorta, spleen, small intestine, or large intestine at the different grasping forces.

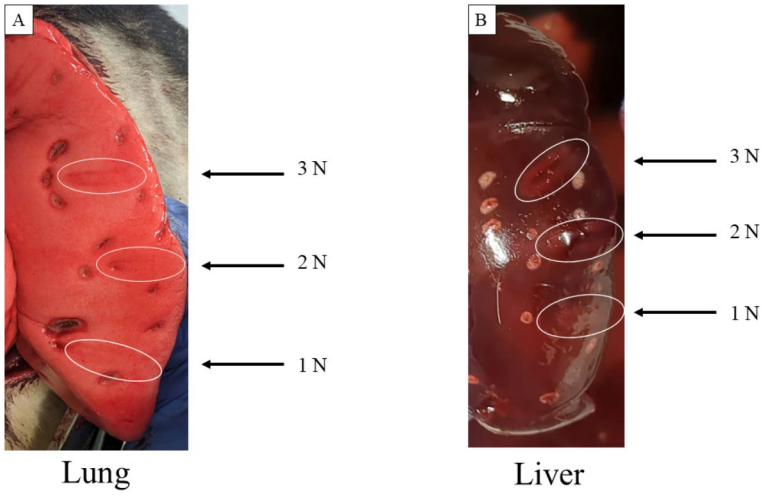

Fig. 3. Macroscopic findings after grasping the (**A**) Lung and (**B**) Liver. The grasped areas of the lung and liver show hemorrhage and congestion that increased at higher grasping forces.

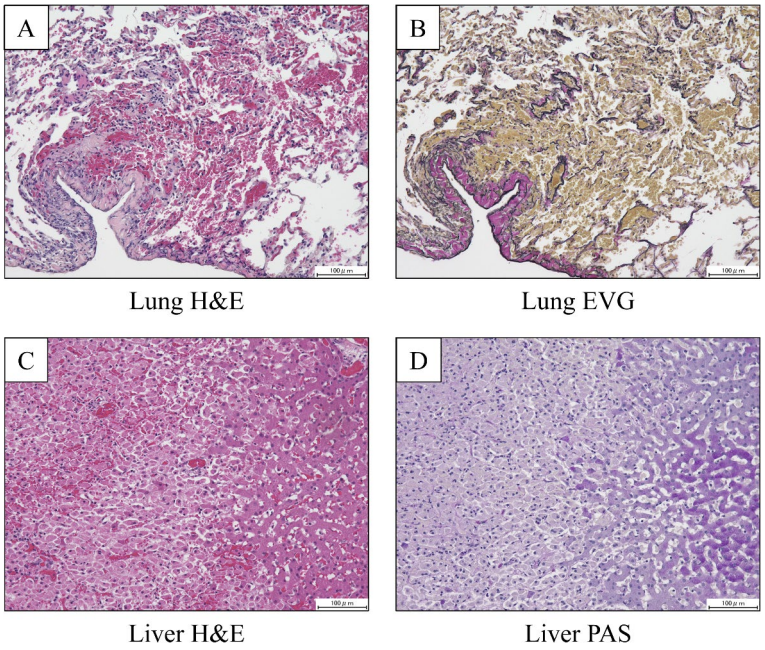

Fig. 4. Histological images of grasped areas in the lung (**A**, **B**) and liver (**C**, **D**). **A** Lung tissue shows hemorrhage and congestion in the grasped areas (H&E staining). **B** Thickness of the pleural elastic and collagen layers increased after grasping (EVG staining). **C** Left half (grasped area) of the liver tissue shows hemorrhage, congestion, and hepatocyte degeneration (H&E staining). **D** The same grasped area in the left half of **C** shows reduced glycogen (PAS staining).

In addition, no major differences in macroscopic findings were noted among the different grasping durations in all organs.

Histological evaluation of tissue damage

Figure 4 shows the histological changes in the lung and liver after the grasping experiments. The lung tissue exhibited hemorrhage and congestion in the grasped areas (Fig. 4A). No morphological irregularities were detected in the alveoli, pleural elastic layers, or collagen layers; however, the thickness of the pleural elastic and collagen layers increased in the grasped areas at higher grasping forces (Fig. 4B). Similarly, the liver tissue exhibited hemorrhage, congestion, and degenerative changes in the grasped areas (Fig. 4C). The degenerative changes included hepatocyte atrophy, impaired adhesion, reduced eosinophilic granularity, pyknosis, and karyorrhexis. A reduction in glycogen was also observed in the grasped areas of the liver (Fig. 4D). No histological

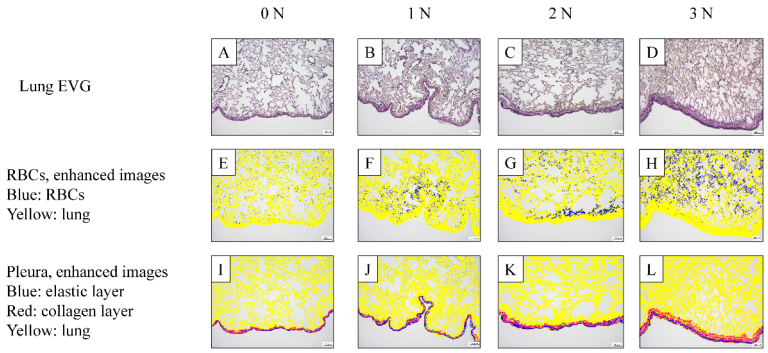

Fig. 5. Histological images of grasped areas in the lung. **A–D** EVG staining. **E–H** Enhanced images of RBCs. Blue: RBCs, Yellow: lung parenchyma. **I–L** Enhanced images of pleural elastic/collagen layers. Blue: elastic layer, Red: collagen layer, Yellow: lung parenchyma.

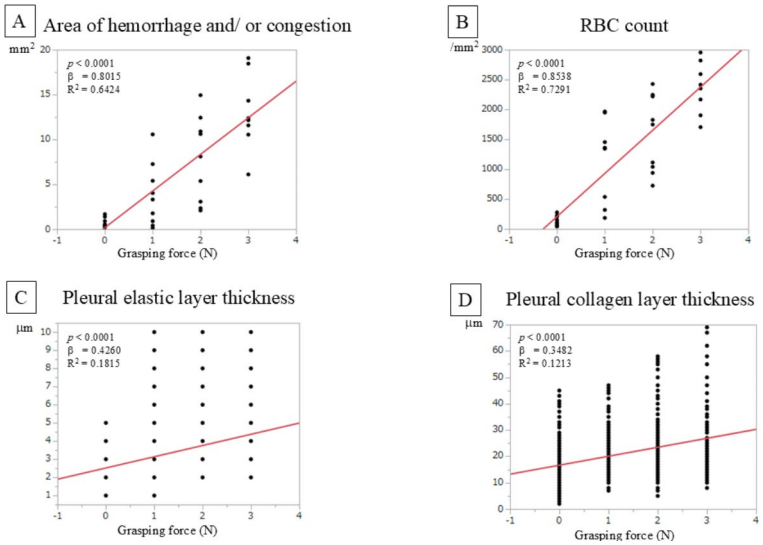

Fig. 6. Results of linear regression analysis of lung tissue damage at different grasping forces. The graphs show the associations between grasping forces and **A** Area of hemorrhage and/ or congestion, **B** RBC count, **C** Pleural elastic layer thickness, and **D** Pleural collagen layer thickness.

changes were observed in the esophagus, aorta, spleen, small intestine, or large intestine at the different grasping forces (Supplementary Fig. 1). Furthermore, no major differences in histological findings were noted among the different grasping durations in all organs.

Associations between lung tissue damage and grasping forces

In grasped lung tissue, the area of hemorrhage and/ or congestion, and RBC count were observed to increase with higher grasping forces (Fig. 5). In addition, the thickness of the pleural elastic layers and collagen layers increased slightly at higher grasping forces. The regression analysis showed that grasping force was significantly and positively associated ($p < 0.0001$) with lung tissue damage (Fig. 6). Specifically, grasping force was strongly associated with the area of hemorrhage and/ or congestion ($\beta = 0.8015$, $R^2 = 0.6424$), and RBC count ($\beta = 0.8538$, $R^2 = 0.7291$), and weakly associated with the thickness of the pleural elastic layers ($\beta = 0.4260$, $R^2 = 0.1815$) and collagen layers ($\beta = 0.3482$, $R^2 = 0.1213$). Post hoc power analysis for the sample size of lung tissue damage, all of parameter were confirmed to exceed 0.8.

Associations between liver tissue damage and grasping forces

In grasped liver tissue, the area of hemorrhage and/ or congestion, RBC count, and area of hepatocyte degeneration were observed to increase with higher grasping forces (Fig. 7). The regression analysis showed that grasping force was significantly and positively associated ($p < 0.0001$) with liver tissue damage (Fig. 8). Specifically, grasping force was strongly associated with the area of hemorrhage and/ or congestion ($\beta = 0.9733$, $R^2 = 0.9475$), RBC count ($\beta = 0.9622$, $R^2 = 0.9260$), and area of degeneration ($\beta = 9153$, $R^2 = 0.8378$). Post hoc power analysis for the sample size of liver tissue damage, all of parameter were confirmed to exceed 0.8.

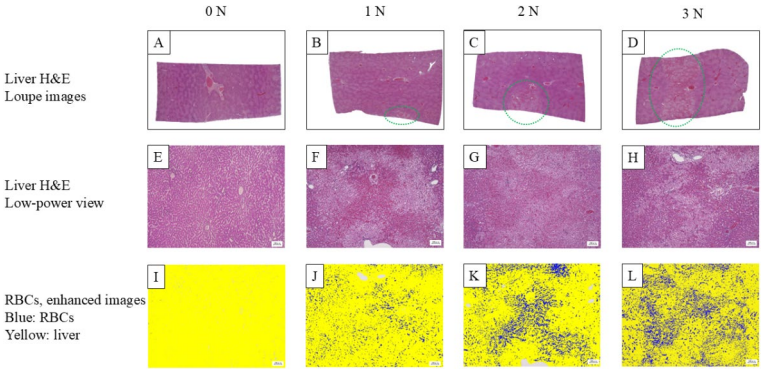

Fig. 7. Histological images of grasped areas in the liver. **A–D** Loupe images in which the dotted lines indicate areas of tissue degenerative change that became more severe as grasping force increased (H&E staining). **E–H** Low-power magnification of the areas shown in **A** to **D**. **F** to **H** correspond to the areas within the dotted lines shown in **B** to **D**. **I–L** Enhanced images of RBCs. Blue: RBCs, Yellow: liver parenchyma.

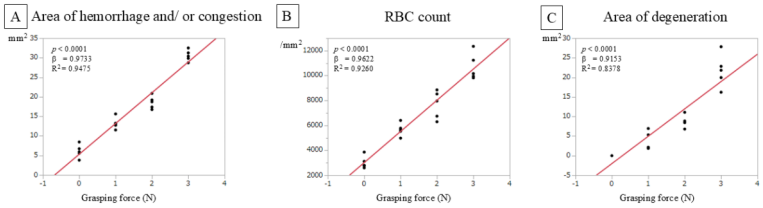

Fig. 8. Results of linear regression analysis of liver tissue damage at different grasping forces. The graphs show the associations between grasping forces and (**A**) Area of hemorrhage and/ or congestion, (**B**) RBC count, and (**C**) Area of degeneration.

Discussion

RAS has been employed in various surgical fields, and the number of RAS cases has steadily increased[6,8]. The advantages of RAS include 3D visualization, elimination of the fulcrum effect and physiological tremors, improvements in ergonomic position, as well as the abilities to scale movements into micromotions, construct microanastomoses, and perform telesurgery[12]. However, these advantages are offset by the absence of tactile sensation, high start-up and running costs, and requirements for additional staff. Furthermore, RAS-associated organ damage can occur due to complications such as incorrect patient positioning, robot malfunction, and lack of tactile sensation[25]. While surgeons may attempt to overcome the lack of tactile sensation through visual cues and other techniques, these abilities are likely to vary among individuals. As a result, organ damage can occur during RAS when tissue is grasped with excessive force[16]. We have previously reported that tissue can be grasped with lower forces during surgical operations using the haptic feedback function of the Saroa surgical system, and that operators can adjust the grasping force as desired to ensure smoothly operation[26]. In that study, we demonstrated that the grasping force exerted on a pig lung was significantly reduced when haptic feedback was engaged. In addition, we showed that procedures such as interlobar dissection, vascular dissection, bronchial dissection, and lymph node dissection could be safely performed with a grasping force of ≤ 3 N. On the other hand, Saroa have haptic feedback of grasping forces, Da Vinci 5 and Senhance have feedback functions of propulsive and traction force, and the reduction of complications is expected even in surgeries using for these functions[27,28]. In addition, not only robotic surgery but also laparoscopic studies are being conducted to introduce tactile feedback and contribute to the reduction of complications[29].

Our present study found significant associations between grasping force and tissue damage in the lung and liver. Although there were associations between grasping force and the thickness of the pleural elastic and collagen layers, the standardized regression coefficients and R^2 values were small and the associations were weak. This may have been due to the inherent thinness of these layers, resulting in a small range of values.

The liver showed an increasing degree of tissue damage, such as hemorrhage and congestion, and degenerative changes, as grasping force increased. Liver injuries can usually be repaired as it is a regenerative organ, and hepatocytes have well-established mechanisms of regeneration when they have normal proliferative capacity. However, severe acute or chronic liver injury can impair the organ's regenerative capabilities. Impaired native hepatocyte regeneration may result in fibrosis, transdifferentiation, and malignant transformation due to DNA damage[30,31]. In order to promote the normal regeneration of hepatocytes, it is important to perform surgeries with the minimum necessary amount of grasping force.

Our experiments did not detect any notable tissue damage in the esophagus, aorta, spleen, small intestine, or large intestine at different grasping forces, which may be due to the mechanical strength of these tissues. For

example, the gastrointestinal tract is thought to have robust tissues because of its well-developed muscular layer, the spleen is maintained in its tissue architecture by the splenic column, and the aorta is rich in elastic fibers. These characteristics may explain the lack of differences in the degree of tissue damage at grasping forces ≤ 3 N. Since Saroa grasps with a force of ≤ 3 N when the haptic feedback function is engaged, we consider that this system can be safely used to operate on these organs.

A limitation of this study is that we were unable to perform subsequent analyses of the damaged tissue. This was because closing the chest after the initial experiment and performing re-thoracotomy would be highly invasive and traumatic to the animal. Accordingly, this was not allowed by the Animal Experimental Committee with consideration to animal welfare.

Our study showed that lung and liver tissue damage occurred even at grasping forces ≤ 3 N, and that higher grasping forces resulted in more severe tissue damage. On the other hand, the haptic feedback function of the Saroa surgical system was shown to enable grasping at a reduced force. These functions could contribute to reduce intraoperative organ damage during lung and liver surgeries.

Data availability

The datasets generated during and/ or analysed during the current study are available from the corresponding author on reasonable request.

Received: 26 December 2024; Accepted: 20 March 2025
Published online: 24 March 2025

References

1. Kwoh, Y. S., Hou, J., Jonckheere, E. A. & Hayati, S. A robot with improved absolute positing accuracy for CT guided stereotactic brain surgery. *IEEE Trans. Boimed Eng.* **35**, 153–160 (1988).
2. Diana, M. & Marescaux, J. Robotic surgery. *Br. J. Surg.* **102**, e15–e28 (2015).
3. Leal Ghezzi, T. & Campos Corleta, O. 30 years of robotic surgery. *World J. Surg.* **40**, 2550–2557 (2016).
4. Lane, T. A short history of robotic surgery. *Ann. R Coll. Surg. Engl.* **100**, 5–7 (2018).
5. Marescaux, J. & Seeliger, B. Robotic surgery: A time of change. *Update Surg.* **75**, 793–794 (2023).
6. Hoeppner, J. Robotic cancer surgery. *Cancers (Basel)* **13**, 3 (2021).
7. Guthart, G. S. & Salisbury, J. K. The Intuitive/sup TM/telesurgery system: Overview and application. In *Proceedings. Millennium Conference. IEEE International Conference on Robotics and Automation 2000* 618–621. (2000).
8. Intuitive Surgical. Annual Report 3–4 (Sunnyvale (CA)). (2023).
9. Ma, J. et al. Robot-assisted thoracic surgery versus video-assisted thoracic surgery for lung lobectomy or segmentectomy in patients with non-small cell lung cancer: A meta-analysis. *BMC Cancer*. **21**, 498 (2021).
10. Cerfolio, R., Louie, B. E., Farivar, A. S., Onaitis, M. & Park, B. J. Consensus statement on definitions and nomenclature for robotic thoracic surgery. *J. Thorac. Cardiovasc. Surg.* **154**, 1065–1069 (2017).
11. Du, H. & Li, H. Robotic thoracic surgery: S1 + 2 segmentectomy of the left upper lobe: Advantage of robotic assisted thoracic surgery. *J. Thorac. Dis.* **9**, E973 (2017).
12. Lanfranco, A. R., Castellanos, A. E., Desai, J. P. & Meyers, W. C. Robotic surgery: A current perspective. *Ann. Surg.* **239**, 14–21 (2004).
13. Toledo, L., Gossot, D., Fritsch, S., Revillon, Y. & Reboulet, C. Study of sustained forces and the working space of endoscopic surgery instruments. *Ann. Chir.* **53**, 587–597 (1999).
14. Karponis, D., Koya, Y., Miyazaki, R., Kanno, T. & Kawashima, K. Evaluation of a pneumatic surgical robot with dynamic force feedback. *J. Robot Surg.* **13**, 413–421 (2019).
15. Trejos, A. L., Patel, R. V. & Naish, M. D. Force sensing and its application in minimally invasive surgery and therapy: A survey. *Proc. Inst. Mech. Eng. C.* **224**, 1435–1454 (2010).
16. Mucksavage, P. et al. Differences in grip forces among various robotic instruments and Da Vinci surgical platforms. *J. Endourol.* **25**, 523–528 (2011).
17. Zhou, D., Tadano, K. & Haraguchi, D. Motion control and external force estimation of a pneumatically driven multi-dof robotic forceps. *Appl. Sci.* **10**, 3679 (2020).
18. Wottawa, C. R. et al. Evaluating tactile feedback in robotic surgery for potential clinical application using an animal model. *Surg. Endosc.* **30**, 3198–3209 (2016).
19. Chen, C. H., Chen, H. H. & Liu, W. M. Complication reports for robotic surgery using three arms by a single surgeon at a single institution. *J. Minim. Access. Surg.* **13**, 22–28 (2017).
20. Maerz, D. A., Beck, L. N., Sim, A. J. & Gainsburg, D. M. Complications of robotic-assisted laparoscopic surgery distant from the surgical site. *Br. J. Anaesth.* **118**, 492–503 (2017).
21. Ackerman, S. J. et al. Comparison of complication and conversion rates between robotic-assisted and laparoscopic rectal resection for rectal cancer: Which patients and providers could benefit most from robotic-assisted surgery? *J. Med. Econ.* **21**, 254–261 (2018).
22. Kapur, A. & Kapur, V. Robotic surgery: Anaesthesiologist's contemplation. *Malays J. Med. Sci.* **27**, 143–149 (2020).
23. Fotiou, A. & Iavazzo, C. Gynecologic robotic surgery: Intraoperative complication and conversion rates. *J. Invest. Surg.* **35**, 916–917 (2022).
24. Buli, B., Diriba, T., Tesfaye, B. & M. & Magnitude of position-related soft tissue injuries and associated factors among elective adult surgical patients at Tikur Anbessa specialized hospital, addis Ababa, Ethiopia. *Ann. Med. Surg. (Lond).* **82**, 104592 (2022).
25. Jara, R. D., Guerrón, A. D. & Portenier, D. Complications of robotic surgery. *Surg. Clin. North. Am.* **100**, 461–468 (2020).
26. Ueda, Y. et al. Impact of a pneumatic surgical robot with haptic feedback function on surgical manipulation. *Sci. Rep.* **13**, 22615 (2023).
27. Gamal, A. et al. Comparing the technological and intraoperative performances of Da Vinci Xi and davinci 5 robotic platforms in patients undergoing robotic-assisted radical prostatectomy. *Eur. Urol. Open. Sci.* **69**, 1–4 (2024).
28. Fujii, T. et al. Comparison of short- and mid-term outcomes between the Senhance digital laparoscopic system and laparoscopic colectomy: A propensity score matching study. *Surg. Endosc.* **39**, 1153–1159 (2025).
29. Hao, Y. et al. Development of force sensing techniques for robot-assisted laparoscopic surgery: A review. *IEEE Trans. Med. Rob. Bionics*. **6**, 868–887 (2024).
30. Gadd, V. L., Aleksieva, N. & Forbes, S. J. Epithelial plasticity during liver injury and regeneration. *Cell. Stem Cell.* **27**, 557–573 (2020).
31. Deng, X. et al. Chronic liver injury induces conversion of biliary epithelial cells into hepatocytes. *Cell Stem Cell* **23** 114–122.e3 e113 (2018).

Acknowledgements
The authors thank Yasushi Tanaka of Riverfield Inc. for contributing to the analysis and assisting in the preparation of the manuscript.

Author contributions
H.N. wrote the main manuscript and prepared all figures. All authors reviewed the manuscript.

Funding
This work was partly supported by a fund for collaborative research between Fukuoka University and Riverfield Inc.

Declarations

Competing interests
Hiroyasu Nakashima, Yuichiro Ueda, and Toshihiko Sato have received research expenses from Riverfield Inc. Yoko Miyanari, Makoto Hamasaki, Makoto Ohbu, Hajime Yamakage, So Miyahara, Keita Tokuishi, Ryuichi Waseda, and Takeshi Shiraishi have no conflicts of interest or financial ties to disclose. Kenji Kawashima is the founder and stockholder of Riverfield Inc. Teruyuki Nishihara is an employee and stock option holder of Riverfield Inc., which is the manufacturer of the Saroa surgical system used in this study.

Additional information
Supplementary Information The online version contains supplementary material available at https://doi.org/10.1038/s41598-025-95310-5.

Correspondence and requests for materials should be addressed to H.N.

Reprints and permissions information is available at www.nature.com/reprints.

Publisher's note Springer Nature remains neutral with regard to jurisdictional claims in published maps and institutional affiliations.